Ultrasmall Fluorescent Ion-Exchanging Nanospheres Containing Selective Ionophores

ARTICLE *in* ANALYTICAL CHEMISTRY · SEPTEMBER 2013

Impact Factor: 5.64 · DOI: 10.1021/ac402564m · Source: PubMed

3 AUTHORS:

Xiaojiang Xie
University of Geneva
32 PUBLICATIONS **277** CITATIONS
SEE PROFILE

Günter Mistlberger
Graz University of Technology
38 PUBLICATIONS **516** CITATIONS
SEE PROFILE

Eric Bakker
University of Geneva
291 PUBLICATIONS **13,818** CITATIONS
SEE PROFILE

analytical chemistry

Article

pubs.acs.org/ac

Ultrasmall Fluorescent Ion-Exchanging Nanospheres Containing Selective Ionophores

Xiaojiang Xie, Günter Mistlberger, and Eric Bakker*

Department of Inorganic and Analytical Chemistry, University of Geneva, Quai Ernest-Ansermet 30, CH-1211 Geneva, Switzerland

Supporting Information

ABSTRACT: We present a convenient precipitation procedure to fabricate ultrasmall fluorescent ion-selective nanosensors that operate on the basis of bulk ion-exchange sensing principles. The nanosphere matrix is composed of bis(2-ethylhexyl) sebacate (DOS) and a triblock copolymer Pluronic® F-127, which also functions as a surfactant to stabilize the nanoparticle. The particles can be prepared easily in large quantity without resorting to further complicated purification. Dynamic light scattering shows that these particles have a monodisperse size distribution with an average diameter of ∼40 nm, suggesting that the nanoparticles are among the smallest ionophore-based ion-selective nanosensors reported to date. A newly reported oxazinoindoline (Ox) as well as a Nile blue derivative (chromoionophore I) was used as a chromoionophore. Na^+- and H^+-selective nanospheres were characterized by absorbance and fluorescence spectroscopy. Owing to the very small size of the nanospheres, the suspension containing the particles is transparent. In the additional presence of the pH indicator HPTS, spectroscopic interrogation of pH and Na^+ in the same sample was demonstrated. As an example, the nanospheres were used to measure the Na^+ level in commercial mineral waters, and the results showed good agreement with atomic absorption spectroscopy (AAS).

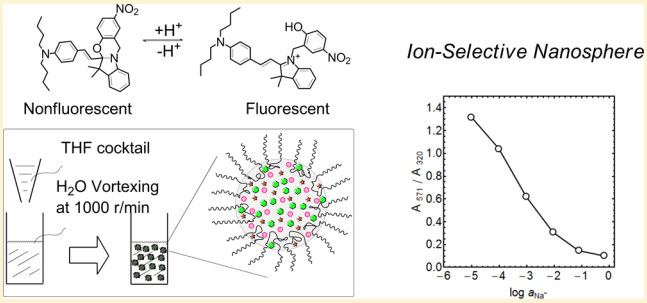

There is an ongoing search to develop sensing strategies for small inorganic ions because they are nutritionally and biologically essential. The fact that they are not biodegradable and remain in ecological systems has made their natural levels important aspects in environmental monitoring. The analysis of ions largely relies on electrochemical methods and optical sensors, followed by atomic (flame) emission spectrometry (AES), atomic absorption spectrometry (AAS), as well as fluorimetry and capillary electrophoresis (CE).[1−8] Although electrochemical methods such as potentiometry, voltammetry, and coulometry are very sensitive, miniaturization is difficult and limits their application in small biological samples such as single cells. Ion-selective microelectrodes have been used to directly measure intracellular concentrations of common inorganic ions.[9−11] However, they assess ion concentration only at a single location in the cell, tend to be noisier and more difficult to handle than larger, more traditionally sized ion-selective electrodes, and require a reference electrode to be inserted at the point of measurement.

Optical sensors are advantageous in this regard because they are easier to miniaturize, and in principle, they are suitable for chemical imaging applications. Ion-selective indicators, whose light emission reflects the local concentration of the ion, have been used for this purpose. Examples include indo-1, rhod-2, and fluo-3 for Ca^{2+}, lucigenin and SPQ (M-440) for Cl^-, and Sodium Green for Na^+.[12−16] Although these indicators are widely used, they suffer from some drawbacks such as cytotoxicity, heavy metal interference (i.e., selectivity), dye leakage, and sequestration.[17] Moreover, their synthesis is difficult, making these compounds expensive. Experiments with large amounts of these indicators can be very costly.

The palette of detectable ions can be expanded with ion-selective optodes, which work on the principle of partitioning of ions between the sample and a sensing phase.[1,18] The above-mentioned ion-selective indicators are not required. These sensors normally contain a lipophilic pH indicator (also called chromoionophore), an ion exchanger, and an ionophore (chemical receptor) for the ionic analyte. These are embedded in a polymeric matrix such as plasticized poly(vinyl chloride) (PVC). The protonation degree of the chromoionophore in the sensing phase reflects the concentration of the analyte in the sample phase and the sample pH.[18] Compared with the above-mentioned ion indicators, the sensor response range is tunable through variation of the optode composition, and the selectivity is often superior owing to the use of very selective ionophores.

Recently, miniaturized forms of the bulk optode have emerged, and microtiter-plate-based optodes, microbeads, and nanospheres have also been prepared by surface coating, polymerization, and sonication.[19−22] Our group has been developing polymeric microspheres that behave on the same basis of bulk ion-selective optodes. Monodisperse optical ion-selective microspheres have been successfully developed through heterogeneous polymerization, solvent casting, or

Received: August 12, 2013
Accepted: September 10, 2013
Published: September 10, 2013

   dx.doi.org/10.1021/ac402564m | Anal. Chem. 2013, 85, 9932−9938

using a sonic particle caster.[20,23−25] It is known that for ion-selective bulk optodes and their ion-selective electrode (ISE) counterparts, electroneutrality of the sensing phase must hold.[18] While for an extremely thin membrane, such as a lipid bilayer, electroneutrality can be partially violated. Previous theoretical work on ISEs indicates a membrane thickness reduction to around 30 nm results in electroneutrality no longer being applicable.[26] Will ultrasmall bulk optodes with sizes of less than 50 nm still be functional? If so, will they work on the same basis as expected from bulk optode theory? These questions are not yet answered since the reliable production of ultrasmall nanospheres has been difficult using existing techniques. The group of Kopelman has reported both acrylamide and PVC-type nanometer-sized sensing spheres that proved to be useful in interrogating intracellular environments.[17,19,27,28] The probes encapsulated by biologically localized embedding (PEBBLE) nanosensors have a bimodal size distribution, and their preparation requires polymerization followed by further purification, which is laborious and time-consuming.[19] Some other nanosensors relying on other materials such as quantum dots and metal beads have also been reported. Nevertheless, the most widely adopted approaches are based on polymeric and sol−gel matrix.[29−32]

In this work, we present a very simple and convenient method to produce monodisperse ultrasmall ion-selective nanospheres (40 nm in diameter). The nanosensor can be produced easily by injection of a tetrahydrofuran (THF) solution containing the sensing components into deionized water. A nonionic, highly biocompatible surfactant triblock copolymer referred to as Pluronic® F-127 (F127) is dissolved in the cocktail. It is composed of a central hydrophobic chain of poly(propylene oxide) flanked by two hydrophilic chains of poly(ethylene glycol) (PEG). F127 plays an important role in the formation of the nanospheres as evidenced by a dual nanosensor for pH and O_2 recently reported using F127, where micelles were formed with F127 and the sensing components, followed by silica growth on the surface.[33] We postulate here that the hydrophobic poly(propylene oxide) chains can interact with other hydrophobic sensing components to help construct the core of the ion-selective nanosphere, while the hydrophilic PEG chains may act as surfactant to prevent the nanosensors from coalescing. These ultrasmall nanospheres are found to be stable, versatile, and easy to fabricate. This allows them to be powerful nanoscale tools to detect small inorganic ions, and they will likely find application in chemical biology and environmental science. Using Na^+ as an example, we incorporate here a neutral Na^+-selective ionophore into the nanospheres, making them sensitive and selective to Na^+. As an early application, the Na^+ concentration in three different commercial mineral water samples was successfully measured using the Na^+-selective nanospheres.

EXPERIMENTAL SECTION

Reagents. Pluronic® F-127 (F127), bis(2-ethylhexyl) sebacate (DOS), sodium ionophore X (NaX), boric acid, tetrahydrofuran (THF), potassium tetrakis-[3,5-bis-(trifluoromethyl)phenyl]borate (KTFPB), 2-amino-2-hydroxymethyl-propane-1,3-diol (Tris), poly(vinyl chloride) (PVC), chromoionophore I (CH1), 8-hydroxypyrene-1,3,6-trisulfonic acid trisodium salt (HPTS), sodium chloride (NaCl), and sodium phosphate monobasic (NaH_2PO_4) were obtained from Sigma-Aldrich. Polyethylene glycol (PEG) was purchased from AppliChem. Mineral water was obtained from Coop®. (*E*)-*N*,*N*-Dibutyl-4-(2-(6,6-dimethyl-2-nitro-6,12-dihydro-5a*H*-benzo[5,6][1,3]oxazino[3,2-a]indol-5a-yl)vinyl)aniline (Ox) was synthesized according to synthesis of similar compounds in a previous report.[34]

Preparation of Ion-Selective Nanospheres. To 3 mL of THF were dissolved 1.81 mg of KTFPB, 0.53 mg of Ox (or 0.58 mg of CH1), 8 mg of DOS, 25 mg of F127, and 2.5 mg of sodium ionophore X (NaX) to form a homogeneous solution. A portion (0.5 mL) of the solution was pipetted and injected into 4.5 mL of deionized water on a vortex with a spinning speed of 1000 r/min. The resulting clear mixture was blown with condensed air on the surface for 20 min to remove THF and gave a clear particle suspension (Table 1E). Other particles shown in Table 1 were prepared in the same way with THF cocktail with different composition and water solution containing the corresponding surfactant. (A) 0.67 mg of PVC and 1.33 mg of DOS into 4.5 mL of 3% (w/w) PEG solution. (B) 0.67 mg of PEG and 1.33 mg of DOS into 4.5 mL of 3% (w/w) PEG solution. (C) 1.33 mg of DOS into 4.5 mL of deionized water. (D) 1.33 mg of DOS and 4.2 mg of F127 into 4.5 mL of deionized water. (F) 1.33 mg of DOS into 4.5 mL 10% (w/w) F127 solution.

Table 1. Average Diameter and Polydisperse Index (PDI) for Particles Precipitated in Different Ways

	sequences	z-av/nm	PDI
A	PVC−DOS in PEG	150 ± 2	0.07 ± 0.03
B	PEG−DOS in PEG	372 ± 8	0.7 ± 0.05
C	PEG−DOS in H_2O	1100 ± 300	0.85 ± 0.04
D	F127−DOS in H_2O	61 ± 1	0.08 ± 0.01
E	F127−DOS in H_2O[a]	40 ± 1	0.04 ± 0.02
F	DOS in F127	96 ± 1	0.1 ± 0.03

[a]With sensing components as indicated in the Experimental Section.

Instrumentation and Measurements. The size of the nanospheres was measured with a particle size analyzer Zetasizer Nano ZS (Malvern, Inc.). The absorbance was measured with a UV−vis spectrometer (SPECORD 250 plus, Analytic Jena, AG, Germany), and fluorescence was measured with a fluorescence spectrometer (FluoroLog 3, Horiba Jobin Yvon). Calibration curves were measured in 10 mM pH 7.4 Tris-HCl buffer solutions with gradual addition of NaCl. Atomic absorption spectroscopic measurements were carried out on a AA240 FS fast sequential atomic absorption spectrometer (VARIAN, Inc.) using flame atomization in absorbance mode.

For the size variation experiment (Figure 5d), 0.5 mL of the THF cocktail (3 mL) containing 1 mg of KTFPB, 0.56 mg of Ox, 8 mg of DOS, and 13.4 mg of F127 was precipitated into 3 mL of deionized water. The THF cocktail for Figure 5c is 4 times more dilute that that in Figure 5d. The resulting particle suspension suspension was diluted with deionized water, and the size of the nanoparticles was measured with a dynamic light scattering particle size analyzer.

For transmission electron microscopy (TEM) imaging of the nanospheres, the sodium-selective nanosphere suspension was dispersed on to a formvar/carbon film coated TEM grid, counter-stained with uranyl acetate, dried in air, and visualized using a FEI Tecnai G2 Sphera transmission electron microscope.

Sodium levels in mineral water were measured with the nanoparticles in absorbance mode. The ratio of the absorbance

dx.doi.org/10.1021/ac402564m | Anal. Chem. 2013, 85, 9932−9938

at 571 nm over 320 nm was taken for the calibration in a pH 7.4 Tris-HCl buffer solution. Samples were diluted with pH 7.4 Tris-HCl buffer solution to reach the same condition as for the calibration. Calibration was performed with sodium concentration in the range from 0.1 mM to 0.3 mM.

For experiments shown in Figure S2, a 5 mM universal buffer (NaH_2PO_4 + boric acid + citric acid) with 1 μM HPTS and Na^+-selective nanosphere was used. The amount of nanospheres that was added was controlled to obtain comparable absorbance intensity with HPTS. The sample contained 0.1 M LiCl. The Na^+ background was adjusted to be 30 mM and 100 mM in two cases.

RESULTS AND DISCUSSION

Ion-selective optical sensors (optodes) can be more easily miniaturized compared to electrochemical sensors. So far, the procedures to miniaturize these sensors mostly involve sonication, precipitation, or polymerization, followed by purification processes such as dialysis and centrifugation.[19,20,35]

The entire procedures based on polymerization are complicated and time-consuming. A sonic particle caster is able to prepare micrometer-sized particles; however, reducing the size further below 100 nm is very difficult, and the efficiency of this method is low because a large amount of aqueous solution is needed compared with the amount of particles formed.[20,25] Methods based on precipitation are more promising to obtain nanoparticles. To make ion-selective particles, typically, a THF cocktail containing PVC, plasticizer, a chromoionophore, an ion-exchanger, and an ionophore is injected into a vortexing aqueous solution containing a surfactant. The composition of the cocktail is the same as in a bulk optode. As shown in Table 1A, when a cocktail containing PVC−DOS is precipitated in a PEG solution, particles with an average size of 150 nm are obtained. The size of the formed nanoparticles depends on many factors during the precipitation, including the polymer concentration, polymer structure, and vortex speed.[35] Nevertheless, with this method, the size of the particles obtained tends to be above 100 nm. Pluronic® F-127 is an interesting polymer with two distal hydrophilic polyethylene glycol chains connected by a hydrophobic poly(propylene oxide) segment. Its molecular weight is around 12 500 Da. We envision that with such a polymer, it is possible to make more compact nanoparticle structures since it plays both the role of PVC and surfactant. To explain, the PEG chain can act as surfactant, while the poly(propylene oxide) chain is able to insert into the plasticizer and stabilize the core of the nanostructure. Since the PEG chain acts as surfactant, no additional surfactant is needed.

Based on these assumptions (as shown in Scheme 1) a cocktail containing DOS and F127 was dissolved in THF and precipitated in deionized water to obtain a mixture containing the desired nanoparticles. THF was removed after precipitation by simply blowing compressed air onto the mixture surface. As shown in Table 1D, nanoparticles with an average size of ∼60 nm in diameter were obtained. The small polydispersity index (PDI) value indicates that the nanoparticles have a narrow size distribution. Since the nanoparticles are very small, the particle suspension appears as a clear solution. Elevating the polymer concentration can result in larger size particles, as explained in previous reports.[35] For instance, when 0.5 mL of the same THF cocktail was injected into 3 mL of water (instead of 4.5 mL) an average diameter around 130 nm was observed. In contrast with F127-based nanospheres, the suspension that resulted from the

Scheme 1. Representation of the Preparation of Na^+-Selective Nanospheres and the Proposed Microscopic Structure. Gray Spherical Background Represents DOS Acting as a Solvent for Other Components

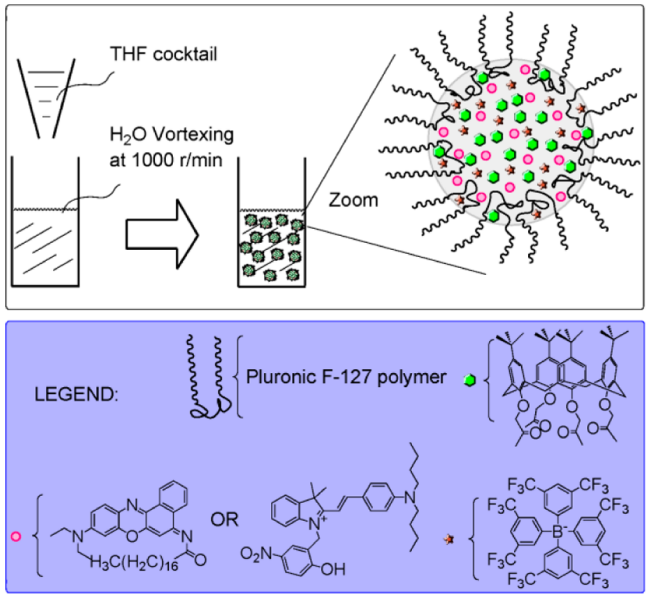

PVC−DOS system contains larger-size particles and appears to be heterogeneous, as evidenced by its ability to scatter light. To confirm that an amphoteric polymer like F127 is essential, PEG was used as a replacement of F127 under the same conditions. The resulting particles showed much larger sizes and PDI values (Table 1C). Even when additional surfactant was used, the size of the particles decreased to around 372 nm but the size distribution range was still wide (Table 1B). When F127 was dissolved in the aqueous solution prior to casting, the resulting nanoparticles still had a small diameter and narrow size distribution, as shown in Table 1F.

With added hydrophobic-sensing components, nanoparticles showed an average hydrodynamic size of 40 nm, as shown in Table 1E. The nanoparticles were also imaged using transmission electron microscopy (TEM). As shown in Figure 1, the

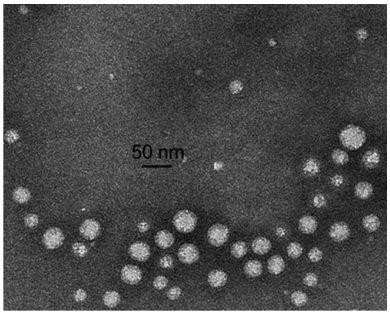

Figure 1. Transmission electron microscopy (TEM) image for the Na^+-selective nanospheres (Table 1E).

nanoparticles exhibited a round shape with a diameter smaller than 40 nm. The size obtained from light scattering measurements is slightly bigger than that observed in TEM because the former technique is dependent on hydrodynamic size.

In a conventional optode, DOS is a very lipophilic molecule and can act as a good solvent for many lipophilic organic

dx.doi.org/10.1021/ac402564m | Anal. Chem. 2013, 85, 9932−9938

molecules. Doping the lipophilic core with a chromoionophore and ion-exchanger should allow the nanoparticles to be pH responsive. To test this, we chose chromoionophore I (CH1), a lipophilic pH indicator, and KTFPB as an ion-exchanger. The pH response of the nanoparticles in absorbance mode is shown in Figure 2. CH1 is a ratiometric dye and indeed shows a visible

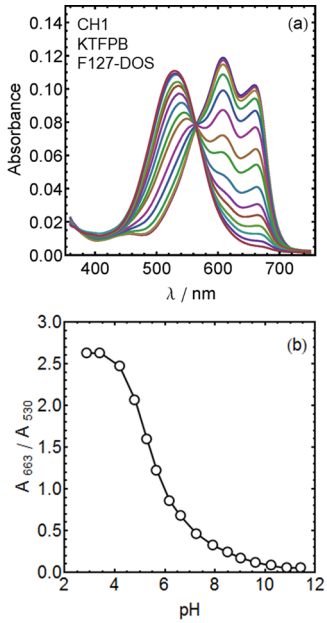

Figure 2. pH response of F127−DOS-based nanospheres containing CH1 and KTFPB in 5 mM universal buffer (NaH_2PO_4 + boric acid + citric acid + 0.1 M KCl). (a) Absorption spectra at different pH. (b) Calibration curve using absorbance ratio between 663 and 530 nm.

response to pH with an isosbestic point at 565 nm. The apparent basicity ($pK_a \simeq 5.9$) of CH1 observed here is lower than in a bulk optode film, indicating that the nanoparticle core and the surface differ in solvent properties such as hydrophobicity, which in turn affects the basicity of the chromoionophore.

One could argue that the chromoionophores are distributed on the surface to equally explain the functioning of the nanosensors and even the reduced basicity. If the chromoionophore is truly inserted into the nanoparticles, protonation should be accompanied by the transfer of a hydrophilic cation (initially ion paired with the ion-exchanger) from the nanospheres to the surrounding solution. For a given pH, the protonation state of the indicator should depend on the nature and concentration of this cation. Therefore, one expects an ion selectivity of the optode response. Consequently, the response of the nanoparticle suspension was evaluated in comparison to different, commonly seen cations. As shown in Figure 3a, without any addition of ionophore, a Hofmeister selectivity series was observed as expected for such an ion-exchange principle, with $K^+ > Na^+ > Mg^{2+} > Ca^{2+}$. With addition of the sodium ionophore NaX, as shown in Figure 3b, the nanoparticles became highly selective for Na^+. This suggests that these nanospheres do indeed behave as bulk extraction systems that do not appear to violate electroneutrality, as expected for ultrasmall dimensions approaching the Debye length.[26] Compared with membrane-based Na^+-selective sensors, the selectivity for Na^+ over K^+ is somewhat reduced due to the different environment of the receptors. Since the

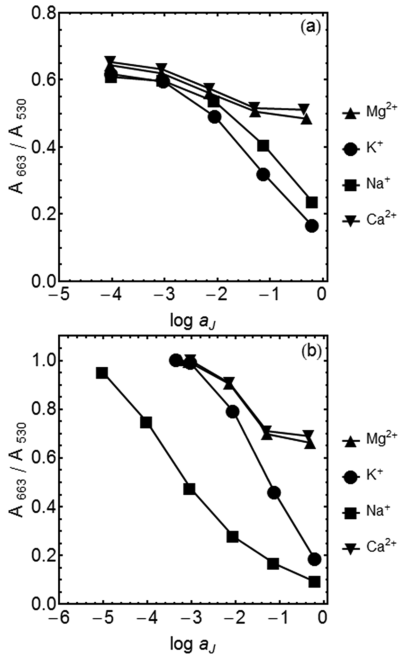

Figure 3. Selectivity for nanospheres comprised of CH1 and KTFPB in 10 mM pH 7.4 Tris-HCl buffer without (a) and with (b) NaX inside the nanosphere.

surface of the nanoparticle is likely more hydrophilic than that of a bulk optode film, a certain leveling effect on the interaction between the ionophore and the metal ion is possible.

The indicator CH1 is not fully protonated under neutral pH conditions, which may be due to its apparently diminished basicity when incorporated into the nanoparticles. To improve on this characteristic, a compound with higher basicity or with lower spectral background when deprotonated (i.e., a turn-on pH indicator) is preferred. Fluorescent probes offer considerable advantages that include a high sensitivity and specificity and versatile measurement parameters (excitation and emission spectra, intensities, lifetimes, or anisotropy). Further Na^+-selective nanoparticles were therefore prepared with a fluorescent turn-on pH sensitive dye, labeled here as Ox, that belongs to a new oxazinoindoline chromoionophore family that we recently introduced.[34] As shown in Figure 4a, Ox can exist in a nonfluorescent ring-closed form and a fluorescent ring-open form. The ring-opening reaction can be mediated by H^+ and renders the dyes pH sensitive. A new Ox dye with enhanced lipophilicity compared with previous work was here synthesized (see Supporting Information for details). Ox is reported to have a higher pK_a than CH1 when interrogated in optical mode.[34] The Na^+ response for this Ox-based nanoparticle is shown in Figure 3. In absorbance mode (Figure 4b,d), the nanoparticles also exhibited a ratiometric response to Na^+. The calibration data does not correspond quantitatively to that expected for a bulk optode, likely because the 40 nm nanosphere size does allow some redistribution of sensing components between surface and bulk during ion exchange (see Figure S1 in Supporting Information).

The Na^+ response of the nanospheres was also evaluated in fluorescence mode, and the results are shown in Figure 4c,e. Error bars are given for three different batches of nanospheres precipitated under identical conditions and indicate that the particles prepared with this method respond in a reproducible fashion. The circles in Figure 4e were measured with particle

dx.doi.org/10.1021/ac402564m | Anal. Chem. 2013, 85, 9932−9938

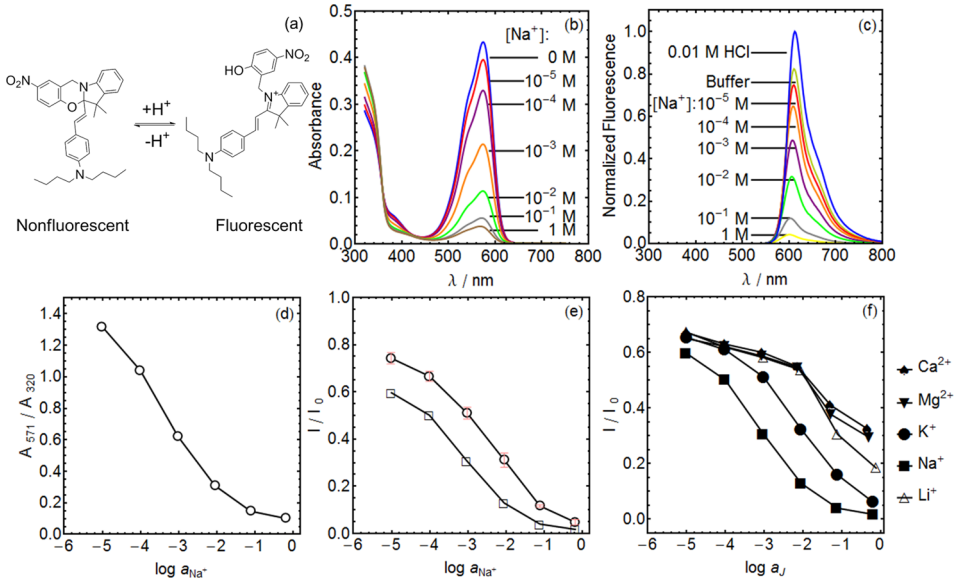

Figure 4. (a) Chemical structure and acid−base reaction of fluorescent turn-on Ox dye. (b) Absorption spectra at various Na^+ concentrations for a Na^+-selective nanoparticle suspension using Ox as chromoionophore in pH 7.4 Tris-HCl buffer, blue line being measured in buffer with no Na^+ as blank. (c) Fluorescence spectra at various Na^+ concentrations for a Na^+-selective nanoparticle suspension using Ox as chromoionophore in pH 7.4 Tris-HCl buffer. (d) Calibration for the Na^+ response in absorbance mode (b) using the absorbance ratio between 571 and 320 nm as output. (e) Circles: Calibration for Na^+ response in fluorescence mode using normalized emission intensity at 610 nm, I_0 being the maximum intensity in 0.01 M HCl (blue line in (c)). Error bars are from three different batches of nanospheres. Squares: Na^+ response obtained with nanosphere suspension diluted 30 times compared with circles. (f) Selectivity of the Na^+-selective nanosphere measured in 10 mM pH 7.4 Tris-HCl buffer solution in fluorescence mode.

suspensions that exhibit the same concentration as for the absorbance data in Figure 4b, while the squares were measured with 30-times-diluted nanoparticle suspensions. We noticed that the concentrated samples give a Na^+ response window that is shifted in the direction of higher Na^+ concentrations, while the response from the diluted suspension is in good agreement with the calibration in absorbance mode.

In principle, this shift could either indicate insufficient stability of the nanoparticles or a modulated fluorescence owing to the high dye concentration. This was evaluated with spectroscopic studies on suspensions of varying dilution. Na^+-selective nanoparticles were prepared and then diluted step-by-step with constant pH (7.4) and a Na^+ (1 mM) background under conditions that are very sensitive to the variation in Na^+ concentration. The relation between the absorbance and the concentrations of the nanosphere remained linear, as shown in Figure S3, indicating that Beer's law still holds throughout the dilution experiment. Should there be a compositional change due to dilution, the Na^+ response, which was evaluated with the absorbance ratio between 571 and 320 nm (A_{571}/A_{320}), would change dramatically. However, as shown in Figure 5a,b, the Na^+ response was stable up to a 40-fold dilution. Evaluation at a stronger dilution was difficult because the absorbance became too low for reliable quantitation (Figure 5a). The size of the nanoparticles with dilution of the suspension was also evaluated using dynamic light scattering and found to be stable. These results suggest that the stability of the nanoparticles is indeed excellent. In fact, these particles can be stored in the dark for more than 4 weeks without noticeable decomposition and sedimentation. Moreover, the photostability of the nanospheres under these experimental conditions is sufficient. As shown in Figure S4, no substantial photobleaching of Ox was seen during a continuous absorbance measurement of 1 h. The selectivity of the Na^+-selective nanoparticles containing Ox was evaluated,

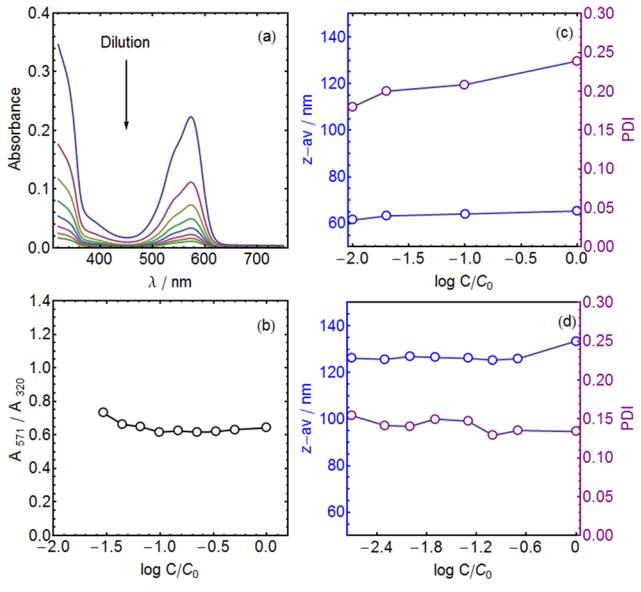

Figure 5. (a) Absorption spectra recorded as the Na^+-selective nanoparticle suspension was diluted with constant Na^+ background (1 mM) and pH (10 mM pH 7.4 Tris-HCl buffer). The dilution factor is indicated on the *x*-axis of Figure 5b. (b) Variation of the Na^+ response with sample dilution. (c) Nanosphere size variation as the particle is diluted with H_2O. Nanospheres were precipitated with THF cocktail containing 1% (w/w) F127−DOS (d) Nanosphere size variation as the particle is diluted with H_2O. Nanospheres were precipitated with THF cocktail containing 4% (w/w) F127−DOS.

and the result is shown in Figure 4f. Similar to the selectivity of CH1-based nanoparticles, Na^+ is highly preferred, while interference from other ions is still suppressed.

dx.doi.org/10.1021/ac402564m | *Anal. Chem.* 2013, 85, 9932−9938

Since the nanoparticle suspension is transparent, it is now possible to measure different parameters in one sample using spectroscopic methods. Here, as a proof of concept, the Na^+-selective nanoparticles and HPTS were simultaneously used to measure Na^+ concentration, as well as pH (Figure S2 in Supporting Information). HPTS was chosen because of its high hydrophilicity and spectral separation with Ox. The pH of the suspension containing a fixed Na^+ concentration (30 mM and 100 mM) was gradually changed while the absorbance signal was recorded. As the pH changes, the degree of protonation $(1-\alpha)$ for both HPTS and Ox in the Na^+-selective nanosphere will vary. However, owing to the ion-exchange reaction between protons and sodium ions, the nanospheres are not only responsive to pH but also to the Na^+ concentration in the sample. Therefore, information concerning both pH and Na^+ concentration can now be revealed at the same time. The ionic strength of the sample was adjusted by addition of LiCl in order to minimize effects of varying activity coefficients on the pH indicator response. As shown in Figure S2, the pH readout from HPTS for samples containing different Na^+ concentrations were the same, while a shift in the degree of protonation for Ox in the nanoparticles is observed, from which the sodium level can be inferred.

As an early stage application, the Na^+-selective nanoparticles were used to measure the sodium concentration in mineral water. Three different commercial mineral water samples were measured with the nanoparticles in absorbance mode, and the results were compared with atomic absorption spectroscopy (AAS). As shown in Table 2, the nanoparticles give very close results compared to AAS. The nanoparticle measurement errors are mainly introduced during the sample preparing stage because a fresh nanoparticle suspension is needed for each measurement.

Table 2. Na^+ Concentrations Assessed in Commercial Water Samples

mineral water brand	AAS/mg L^{-1}	nanoparticle/mg L^{-1}	label/mg L^{-1}
Crystalp	19.3 ± 0.1	19.5 ± 0.9	19.9
Evian	5.9 ± 0.1	5.6 ± 0.5	6.5
Vichy	1010 ± 2	1080 ± 32	1172

CONCLUSION

In conclusion, a simple and convenient method based on precipitation of lipophilic components in H_2O for preparing ion-selective nanoparticles is presented. The preparation process can be finished in less than 30 min and does not require further complicated purifications. Na^+-selective and pH-sensitive nanoparticles incorporating fluorescent turn-on and ratiometric dyes were prepared and studied as model systems. With the help of an amphoteric polymer F127, the nanoparticles exhibit very small size (~40 nm) and a narrow size distribution. Perhaps surprisingly, the nanospheres appear to exhibit selective ion-exchange chemistry, although with response curves that do not quantitatively correspond to bulk optode theory. The resulting particle suspension is transparent and can allow for a spectroscopic interrogation of different parameters at the same time. Na^+ concentrations in commercial mineral waters were successfully determined. The nanoparticles are highly stable upon dilution and long storage. Further work to obtain a deeper understanding of the microscopic structure of the nanospheres and to build nanospheres sensitive and selective to other ions is ongoing in our laboratory.

ASSOCIATED CONTENT

Supporting Information

Additional information as noted in the text. This material is available free of charge via the Internet at http://pubs.acs.org.

AUTHOR INFORMATION

Corresponding Author

*E-mail: eric.bakker@unige.ch.

Notes

The authors declare no competing financial interest.

ACKNOWLEDGMENTS

The authors thank the Swiss National Science Foundation and the University of Geneva for financial support. We are grateful to Dr. István Szilágyi for the help in dynamic light scattering measurements. G.M. gratefully acknowledges the support of the Austrian Science Fund (FWF): J3343.

REFERENCES

(1) Mistlberger, G.; Xie, X.; Pawlak, M.; Crespo, G. A.; Bakker, E. *Anal. Chem.* **2013**, *85*, 2983.
(2) Bakker, E.; Qin, Y. *Anal. Chem.* **2006**, *78*, 3965.
(3) Akcin, N.; Koyuncu, I.; Akcin, G. *Rev. Anal. Chem.* **2011**, *30*, 65.
(4) Li, X.; Zhou, D.; Xu, J.; Chen, H. *Talanta* **2007**, *71*, 1130.
(5) Alvarez, M. A.; Carrillo, G. *Talanta* **2012**, *97*, 505.
(6) Aragay, G.; Pons, J.; Merkoçi, A. *Chem. Rev.* **2011**, *111*, 3433.
(7) Thakur, A.; Mandal, D.; Ghosh, S. *Anal. Chem.* **2013**, *85*, 1665.
(8) Town, R. M.; Leeuwen, H. P. V. *Electroanalysis* **2004**, *16*, 458.
(9) Hu, Z.; Buehrer, T.; Mueller, M.; Rusterholz, B.; Rouilly, M.; Simon, W. *Anal. Chem.* **1989**, *61*, 574.
(10) Chumbimuni-Torres, K. Y.; Dai, Z.; Rubinova, N.; Xiang, Y.; Pretsch, E.; Wang, J.; Bakker, E. *J. Am. Chem. Soc.* **2006**, *128*, 13676.
(11) Wen, R.; O., B., II *J. Neurosci. Meth.* **1990**, *31*, 207.
(12) June, C. H.; Rabinovitch, P. S. *Methods Cell Biol.* **1990**, *33*, 37.
(13) Hamaguchi, Y.; Hamaguchi, M. S.; Mohri, T. *Cell* **1990**, *22*, 258.
(14) Ma, A.; Rosenzweig, Z. *Anal. Chem.* **2004**, *76*, 569.
(15) Bahmanjah, S.; Zhang, N.; Davis, J. T. *Chem. Commun.* **2012**, *48*, 4432.
(16) Kim, M. K.; Lim, C. S.; Hong, J. T.; Han, J. H.; Jang, H.-Y.; Kim, H. M.; Cho, B. R. *Angew. Chem., Int. Ed.* **2010**, *49*, 364.
(17) Si, D.; Epstein, T.; Lee, Y.-E. K.; Kopelman, R. *Anal. Chem.* **2012**, *84*, 978.
(18) Bakker, E.; Bühlmann, P.; Pretsch, E. *Chem. Rev.* **1997**, *97*, 3083.
(19) Clark, H. A.; Hoyer, M.; Philbert, M. A.; Kopelman, R. *Anal. Chem.* **1999**, *71*, 4831.
(20) Tsagkatakis, I.; Peper, S.; Bakker, E. *Anal. Chem.* **2001**, *73*, 315.
(21) Dubach, J. M.; Harjes, D. I.; Clark, H. A. *J. Am. Chem. Soc.* **2007**, *129*, 8418.
(22) Dubach, J. M.; Das, S.; Rosenzweig, A.; Clark, H. A. *Proc. Natl. Acad. Sci. U.S.A.* **2009**, *106*, 16145.
(23) Telting-Diaz, M.; Bakker, E. *Anal. Chem.* **2002**, *74*, 5251.
(24) Retter, R.; Peper, S.; Bell, M.; Tsagkatakis, I.; Bakker, E. *Anal. Chem.* **2002**, *74*, 5420.
(25) Xu, C.; Wygladacz, K.; Retter, R.; Bell, M.; Bakker, E. *Anal. Chem.* **2007**, *79*, 9505.
(26) Morf, W. E.; Pretsch, E.; Rooij, N. F. D. *J. Electroanal. Chem.* **2010**, *641*, 45.
(27) Shortreed, M.; Bakker, E.; Kopelman, R. *Anal. Chem.* **1996**, *68*, 2656.
(28) Park, E. J.; Brasuel, M.; Behrend, C.; Philbert, M. A.; Kopelman, R. *Anal. Chem.* **2003**, *75*, 3784.
(29) Sandros, M. G.; Shete, V.; Benson, D. E. *Analyst* **2009**, *131*, 229.

(30) Aslan, K.; Wu, M.; Lakowicz, J. R.; Geddes, C. D. *J. Am. Chem. Soc.* **2007**, *129*, 1524.
(31) Burns, A.; Sengupta, P.; Zedayko, T.; Baird, B.; Wiesner, U. *Small* **2006**, *2*, 723.
(32) Hammond, V. J.; Aylott, J. W.; Greenway, G. M.; Watts, P.; Webster, A.; Wiles, C. *Analyst* **2008**, *133*, 71.
(33) Wang, X.-D.; Stolwijk, J. A.; Lang, T.; Sperber, M.; Meier, R. J.; Wegener, J.; Wolfbeis, O. S. *J. Am. Chem. Soc.* **2012**, *134*, 17011.
(34) Xie, X.; Crespo, G. A.; Bakker, E. *Anal. Chem.* **2013**, *85*, 7434.
(35) Borisov, S. M.; Mayr, T.; Mistlberger, G.; Waich, K.; Koren, K.; Chojnacki, P.; Klimant, I. *Talanta* **2009**, *79*, 1322.